Molecular Immunology 170 (2024) 99–109

Contents lists available at ScienceDirect

Molecular Immunology

journal homepage: www.elsevier.com/locate/molimm

2-Substituted-4,7-dihydro-4-ethylpyrazolo[1,5-*a*]pyrimidin-7-ones alleviate LPS-induced inflammation by modulating cell metabolism via CD73 upon macrophage polarization

Alessia Ricci [a,1], Susi Zara [a,1], Fabrizio Carta [b], Valentina Di Valerio [c], Silvia Sancilio [d], Amelia Cataldi [a], Silvia Selleri [b], Claudiu T. Supuran [b], Simone Carradori [a], Marialucia Gallorini [a,*]

[a] Department of Pharmacy, University "G. d'Annunzio" of Chieti-Pescara, Chieti 66100, Italy
[b] NEUROFARBA Department, Section of Pharmaceutical and Nutraceutical Sciences, University of Florence, Florence, Italy
[c] Department of Innovative Technologies in Medicine and Dentistry, University "G. D'Annunzio" Chieti-Pescara, Chieti, Italy.
[d] Department of Medicine and Ageing Sciences, University "G. d'Annunzio" of Chieti-Pescara, Chieti 66100, Italy

ARTICLE INFO

Keywords:
Macrophages
Polarization
LPS
Nrf2
CD73
Metabolism
Immunomodulation
Pyrazolo[*l*,5-*a*]pyrimidin-7-ones
Inflammation

ABSTRACT

Macrophage polarization towards the M1 phenotype under bacterial product-related exposure (LPS) requires a rapid change in gene expression patterns and cytokine production along with a metabolic rewiring. Metabolic pathways and redox reactions are such tightly connected, giving rise to an area of research referred to as immunometabolism. A role in this context has been paid to the master redox-sensitive regulator Nuclear factor erythroid 2-related factor 2 (Nrf2) and to the 5'-ectonucleotidase CD73, a marker related to macrophage metabolism rearrangement under pro-inflammatory conditions. In this light, a cell model of LPS-stimulated macrophages has been established and nine 4,7-dihydro-4-ethylpyrazolo[*l*,5-*a*]pyrimidin-7-ones with a potential anti-inflammatory effect have been administered. Our data highlight that two selected compounds (namely, **5** and **8**) inhibit the LPS-induced Nrf2 nuclear translocation and ameliorate the activity rate of the antioxidant enzyme catalase. Additionally, the pyridine-containing compound (**8**) promotes the shift from the pro-inflammatory immunophenotype M1 to the pro-resolving M2 one, by downregulating CD80 and iNOS and by enhancing CD163 and TGFβ1 expression. Most importantly, CD73 is modulated by these compounds as well as the lactate production. Our data demonstrate that pyrazolo[*l*,5-*a*]pyrimidine derivatives are effective as anti-inflammatory compounds. Furthermore, these pyrazolo[*l*,5-*a*]pyrimidines exert their action via CD73-related signaling and modulation of cell metabolism of activated macrophages.

1. Introduction

Macrophages represent the first line of defense within the human body. Being widely distributed in all the anatomical districts, they represent specialized cells committed to the maintenance of tissue homeostasis upon oxidative stress-related inflammation and infections (Shapouri-Moghaddam et al., 2018). Monocytes and macrophages are members of the mononuclear phagocyte system, a component of the innate immunity. Circulating blood monocytes, after sensing chemotactic signals, leave the circulation and migrate into inflamed tissues to differentiate in macrophages (Chiu and Bharat, 2016). The heterogeneity of each macrophage population may reflect the required level of specialization within the environment of any given tissue (Papalexi and Satija, 2018). According to their inflammatory status, macrophages are classified as classically activated (pro-inflammatory, M1), non–activated (M0) and alternatively activated (anti-inflammatory or pro-resolving, M2) cells, a classification also associated with distinct genetic profiles and expression of specific surface markers (Yunna et al., 2020). The M1 activation occurs after tissue injury or stimulation by bacterial products such as lipopolysaccharide (LPS) in a pro-inflammatory environment dominated by Toll-like receptors (TLRs), interferon (IFN) signaling and inducible nitric oxide synthase (iNOS)

* Corresponding author.
E-mail address: marialucia.gallorini@unich.it (M. Gallorini).
[1] These authors contributed equally to the work.

https://doi.org/10.1016/j.molimm.2024.04.004
Received 21 August 2023; Received in revised form 10 March 2024; Accepted 6 April 2024
Available online 20 April 2024

activation (Jiménez-Uribe et al., 2019). In parallel, M2 macrophages mediate wound healing process and resolution of inflammation by producing a range of anti-inflammatory molecules including Transforming growth factor beta 1 (TGFβ1) and interleukin (IL)-10, and by promoting T helper (Th) 2 anti-inflammatory responses (Hassanshahi et al., 2022).

Energy is required to orchestrate the rapid production of pro-inflammatory mediators and activation of phagocytosis in parallel with the M1/M2 transition. Obtaining and maintaining an activated phenotype involve an array of energy-demanding biochemical processes controlled by specific signaling pathways (Kolliniati et al., 2022). There is increasing evidence that different metabolic characteristics and the shift of inflammation phenotypes are highly dependent on Nuclear factor erythroid 2-related factor 2 (Nrf2) in activated macrophages (Wang and He, 2022). Nrf2 is a transcription factor expressed at a low level in the cytoplasm of most tissues and cells under basal conditions. Within the cytoplasm, Nrf2 is bound to the Kelch-like ECH-associated protein 1 (KEAP1). Nrf2 is released in response to pro-oxidant signals sensed by KEAP1, translocates into the nucleus, accumulates, and binds to antioxidant response elements (AREs) of target gene promoters (Nguyen et al., 2009). Murine inflammatory models demonstrated that Nrf2 suppresses inflammation by opposing the transcriptional upregulation of pro-inflammatory cytokine genes and thus interfering with IL-6 induction and inflammatory phenotypes *in vivo* (Kobayashi et al., 2016). Moreover, it directly transcripts for antioxidants enzymes largely involved in the transition from the M1 phenotype to the M2 one (Naito et al., 2014).

Recent studies highlighted the role of aerobic and anaerobic glycolytic metabolism in the activation of innate immune cells (Yu et al., 2020). Upon TLR stimulation, activated immune cells switch their metabolism from oxidative phosphorylation to anaerobic glycolysis, resulting in increased production of lactate (Manoharan et al., 2021) to meet their augmented metabolic requirements and ATP request (Rodríguez-Prados et al., 2010). It has been shown that adenosine triphosphate (ATP) and its catabolic derivatives ADP, AMP, and adenosine, contribute to the immunomodulatory effects on macrophages. The breakdown of extracellular adenine nucleotides (ATP, ADP, AMP) to adenosine is regulated by key ecto-nucleotidases on the macrophage surface, such as CD73 (Murphy et al., 2017). Recently, CD73 has been reported as a crucial protein involved in immunoregulation, playing an essential role in balancing inflammation and immune suppression by converting AMP to adenosine. Importantly, studies have shown that CD73 can modulate tumorigenesis, proliferation, migration, and immune escape, and may be a novel immune regulator in tumor immunotherapy (Tang et al., 2022).

In this context, tuning the pro-oxidant and inflammatory environment by modulating the activation state of macrophages and their metabolism, might be an effective method for the treatment of inflammatory-related diseases and prevention of chronic inflammation through immunotherapy (Li et al., 2022).

Previously, a series of 4,7-dihydro-4-ethylpyrazolo[*l*,5-*a*]pyrimidin-7-ones functionalized with alkyl chains, cycloaliphatic rings, (un) substituted aromatic rings and bioisosteric heterocycles have been synthesized given their inhibitory effects against phosphodiesterases (Bruni et al., 1993). These compounds were also demonstrated to inhibit leukotrienes and/or prostaglandin biosynthesis modulating superoxide production and myeloperoxidase release, to reduce carrageenan-induced rat paw edema and pleurisy *in vivo*, and to display weak acute toxicity. These biological activities were dependent on the substituent at position 2. A more recent analysis of *in silico* prediction also suggested that the iNOS could be one of the targets of this scaffold (in particular for compound **8**) (Daina et al., 2019). To further investigate the anti-inflammatory and antioxidant potential of this series, we have selected the best-in-class compounds of our previously published series. Moreover an ethyl ester carboxylate at position 6 was inserted for the first time to further reinforce the already disclosed structure-activity relationships associated with this scaffold, suggesting that some positions must be left unsubstituted (e.g., 3 and 5) (Fig. 1).

Against this background, a model of LPS-stimulated human macrophages has been established and the previously synthesized compounds were administered in parallel with the nonsteroidal anti-inflammatory drug (NSAID) Meloxicam, as the anti-inflammatory reference compound (Khalil and Aldosari, 2020). The present work therefore aims at evaluating the effectiveness of selected 4,7-dihydro-4-ethylpyrazolo[*l*,5-*a*]pyrimidines in the counteraction of LPS-induced inflammation in terms of cell metabolic activity, generation of reactive nitrogen species (RNS), immunophenotype of activated macrophages and Nrf2 translocation. Additionally, expression levels of proteins related to the increased macrophage metabolism upon the M1/M2 polarization were analyzed.

2. Materials and methods

2.1. Synthesis and characterization of compounds 1-9

Compounds **1**-**8** were synthesized as previously reported (Bruni et al., 1993). Compound **9** was designed and synthesized to assess the importance of the substitution at position 6. Reagents and anhydrous solvents were purchased from Sigma-Aldrich. All reactions involving air- or moisture-sensitive compounds were performed under a nitrogen atmosphere. Nuclear magnetic resonance

^{1}H and ^{13}C spectra were recorded using a Bruker Advance III 400 MHz spectrometer. Chemical shifts are reported in parts per million (ppm) and the coupling constants (J) are expressed in Hertz (Hz). Splitting patterns are designated as follows: s, singlet; t, triplet; m, multiplet. Melting points were measured on a Stuart® melting point apparatus SMP1 and are uncorrected (temperatures are reported in °C). Elemental analyses for C, H, and N were recorded on a Perkin-Elmer 240 B microanalyzer and the analytical results were within ± 0.4 % of the theoretical values. Analytical thin-layer chromatography (TLC) was carried out on Merck silica gel F-254 plates. Flash chromatography purifications were performed on Merck silica gel 60 (230–400 mesh ASTM) as the stationary phase, and ethyl acetate and *n*-hexane were used as eluents. Ethyl 4-ethyl-7-oxo-2-(thiophen-2-yl)-4,7-dihydropyrazolo[1,5-*a*]pyrimidine-6-carboxylate (**9**) was obtained as a white crystals (87% yield), m.p. 219–222 °C.

^{1}H-NMR (DMSO-d_6, 400 MHz) δ (ppm): 1.32–1.35 (t, J = 7.1 Hz, 3 H), 1.44–1.48 (t, J = 7.1 Hz, 3 H), 4.26–4.32 (m, 4 H), 7.10 (s, 1 H), 7.22–7.24 (m, 1 H), 7.70–7.72 (t, J = 3.8 Hz, 1 H), 8.75 (s, 1 H); ^{13}C-NMR (DMSO-d_6, 100 MHz) δ (ppm): 14.5 (CH_3), 15.2 (CH_3), 49.9 (CH_2), 61.0 (CH_2), 89.5 (CH=), 100.5 (CH=), 127.9 (CH=), 128.4 (CH=), 128.9 (CH=), 135.8 (CH=), 143.4 (CH=), 148.8 (CH=), 150.2 (CH=), 153.0 (C═O), 164.2 (C═O). Anal. Calcd for $C_{15}H_{15}N_3O_3S$: C, 56.77; H, 4.76; N, 13.24. Found: C, 56.83; H, 4.79; N, 13.27.

2.2. Cell culture and differentiation

A cell line of undifferentiated human monocytes (CRL-9855™) was purchased from ATCC® and sub-cultured in complete RPMI 1640 (Merck, Darmstadt, Germany) supplemented with 10 % heat-inactivated fetal bovine serum (FBS), 1 % penicillin/streptomycin, and 1 % sodium pyruvate (all from Gibco, Invitrogen, Life Technologies, Carlsbad, CA, USA) at 37 °C and 5 % CO_2.

For differentiation into macrophages, monocytes were seeded in multi-well culture plates and stimulated with 100 ng/mL of PMA (phorbol-12-myristate-13-acetate, purchased from Merck, Darmstadt, Germany, stock solution 1 mM in DMSO) as previously described (Gallorini et al., 2022).

2.3. Cell metabolic activity (MTT test)

Undifferentiated monocytes were seeded (5 ×10^3 cells/well) in 96

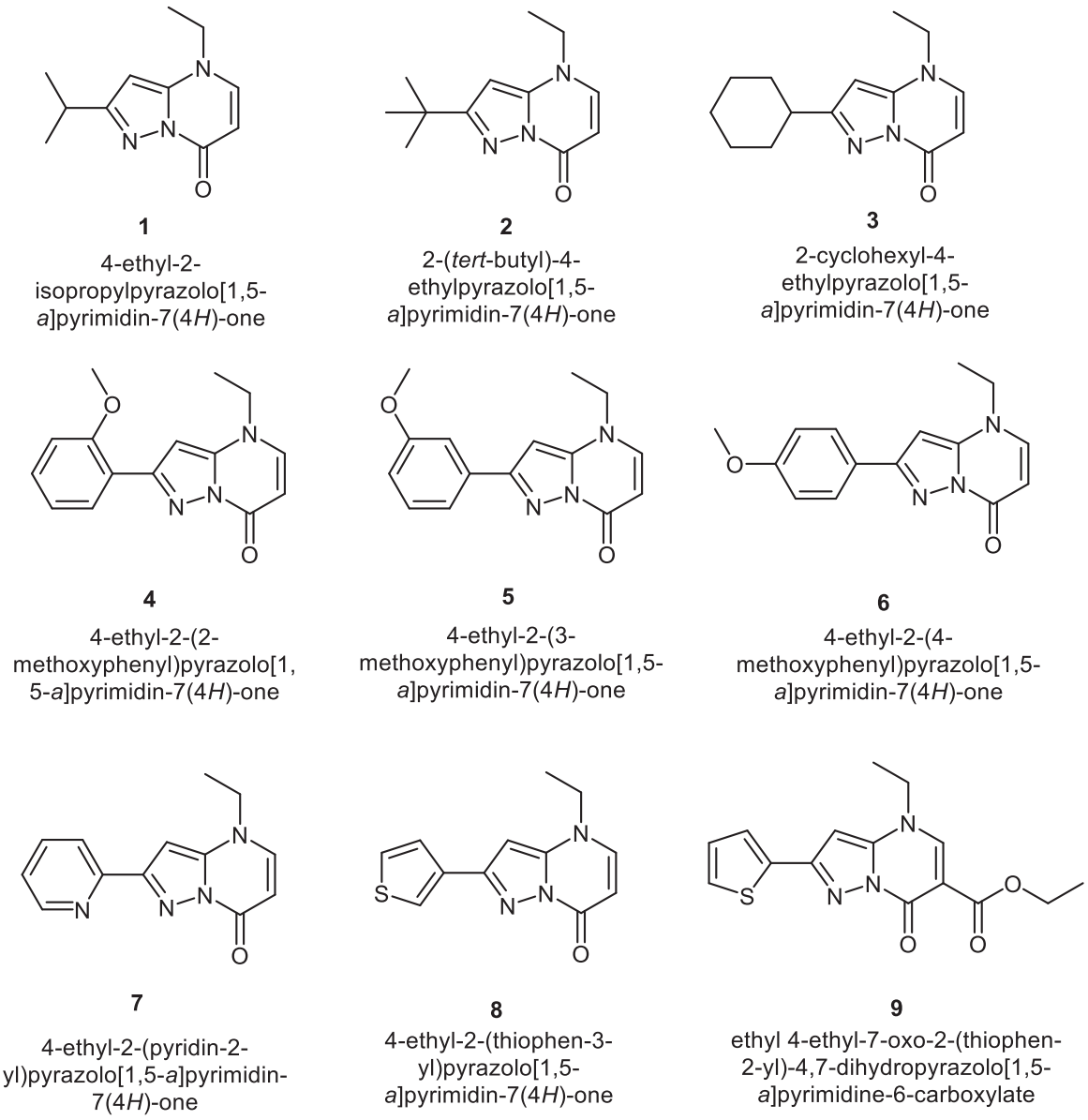

Fig. 1. Selected 4,7-dihydro-4-ethylpyrazolo[*l*,5-*a*]pyrimidin-7-ones assayed in this study.

multi-well culture plates (Corning™ Falcon™, Glendale, USA) and differentiated as described previously in this section (Paragraph 2.2). Then, the differentiation medium was discarded after 48 h and replaced with a fresh one containing complete RPMI (untreated cells = CTRL) or compounds (**1**-**9**) at 1 and 10 μM (stock solution 100 mM in DMSO) or Meloxicam (Merck, Darmstadt, Germany) at 1 and 10 μM (stock solution 100 mM in DMSO). To induce inflammation, macrophages were stimulated with LPS 0.5 μg/mL (lipopolysaccharide from *E. coli*, purchased from Merck, Darmstadt, Germany, stock solution 1 mg/mL in water) and further exposed to compounds (**1–9**) or Meloxicam at 1 and 10 μM.

At the established time point (24 h), the exposure media were replaced by fresh RPMI containing 3-(4,5-dimethylthiazol-2-yl)-2,5-diphenyltetrazolium bromide (MTT) 0.5 mg/mL (Merck, Darmstadt, Germany) and processed as elsewhere reported (Gallorini et al., 2022). The optical density in each well was measured using a spectrophotometer (Thermo Fisher Scientific, Waltham, MA, USA) at a wavelength of 540 nm. Each experiment was performed three times in triplicates per experimental condition (n = 9).

2.4. IL-6 and PGE2 secretion

Cell culture supernatants were collected after 24 h and analyzed for cytokine release. The amounts (pg/mL) of interleukin-6 (IL-6) and prostaglandin E2 (PGE2) were quantified using commercial ELISA kits (Enzo Life Sciences Inc, Lausen, Switzerland) as reported elsewhere (Sancilio et al., 2019).

2.5. Generation of peroxynitrite

Differentiated macrophages (2×10^5 cells/well) were grown, stimulated with LPS, and exposed to compounds **5** and **8** or Meloxicam at 10 μM in 6-well plates. At the established time point (24 h), the DAX-J2™ PON Green probe (Cell Meter™ Fluorimetric Intracellular Peroxynitrite Assay Kit, AAT Bioquest, Pleasanton, CA, USA) was used for detecting the production of peroxynitrite by flow cytometry as described elsewhere (Schweikl et al., 2021). The experiment was performed in triplicate (n = 3). Relative fluorescence emissions of gated cells by means of their forward and side scatter properties (FSC/SSC) were analyzed with the CytExpert software (Beckman Coulter, Indianapolis,

IN, USA), and they were expressed as mean fluorescence intensities (Fluorescence factor) ± standard deviations.

2.6. Protein extraction

Monocytes (1.0×10^6) were differentiated in cell culture plates (100 ×20 mm Petri Dish) at 37 °C and 5 % CO_2 as previously described. Next, differentiated macrophages were cultured in the same experimental conditions of peroxynitrite measurements. After 24 h of treatments, adherent cells were collected by centrifugation. Next, the whole cell fraction was extracted as already reported (Gallorini et al., 2015). The amount of protein present in each cytoplasmic and nuclear fraction was determined by a BCA protein assay (QuantiPro™ BCA Assay kit for 0.5–30 mg/mL protein, Merck, Darmstadt, Germany) following the manufacturer's instructions. The assay was performed in triplicate for each experimental condition (n = 3).

2.7. Immunoblotting

Proteins (20 μg per lane) were first separated on a 4–20 % SDS-PAGE Gel (ExpressPlus™ 10 × 8, GenScript Biotech Corporation, Nanjing, China) and transferred to nitrocellulose membranes at 350 mA for 120 min. Nitrocellulose membranes were then blocked in 5 % of non-fat milk or 5 % of BSA, 10 mmol/L Tris pH 7.5, 100 mM NaCl, 0.1% Tween 20 and probed overnight at 4 °C under gentle shaking with rabbit polyclonal anti-Nrf2 (dilution 1:750) and anti-iNOS primary antibodies, both purchased from Santa Cruz Biotechnology (Santa Cruz, CA, USA); mouse monoclonal anti-TGFβ1 primary antibody (dilution 1:1000) from Abcam (Cambridge, USA); mouse monoclonal anti-β-actin (dilution 1:5000) primary antibody purchased from Merck, Darmstadt, Germany. Afterward, membranes were incubated in the presence of specific IgG horseradish peroxidase (HRP)-conjugated secondary antibodies. Immunoreactive bands were identified using the ECL detection system (LiteAblot Extend Chemiluminescent Substrate, EuroClone S.p.A., Milan, Italy).

2.8. Immunofluorescence staining of Nrf2

Monocytes (0.3×10^5 cells) were seeded on round shaped Thermanox (Thermo Fisher Scientific™, Waltham, MA, USA) and differentiated as previously described. Differentiated macrophages were stimulated with LPS and exposed to Meloxicam and **8** at 10 μM for 24 h. After fixation with 4 % paraformaldehyde and blocking at 37 °C with 10 % normal goat serum/PBS for 30 min, samples were incubated with anti-Nrf2 rabbit polyclonal antibody (Santa Cruz Biotechnology, Santa Cruz, CA, USA) diluted 1:100 in 0.5 % Tween 20 in 2 % BSA/PBS overnight at 4 °C. After several washings with PBS, samples were incubated with a goat anti-rabbit IgG FITC (Jackson Immuno Research, West Grove, PA, USA), diluted 1:50 in 0.5 % Tween 20 in 2 % BSA/PBS for 45 min at 37 °C. Nuclei were counterstained using VECTASHIELD® Antifade Mounting Medium with DAPI (Vector Laboratories, Burlingame, CA, USA). The observations were carried out with a ZEISS Axioskop 40 (Carl Zeiss) light microscope equipped with a Coolsnap VideoCamera. Metamorph (Molecular Devices) software was used for acquiring computerized images, counting cells stained positive for DAPI, Nrf2-FITC and for the quantification of Nrf2 nuclear translocation (merged DAPI and FITC fluorescence).

2.9. Immunophenotyping in vitro

The expression of surface markers (CDs) in both undifferentiated monocytes and differentiated macrophages was analyzed by flow cytometry. After differentiation, macrophages were stimulated with LPS and exposed to compounds **5** and **8** or Meloxicam at 10 μM for 24 h. After that, cells were harvested with Stem Pro™ Accutase™ cell dissociation reagent (ThermoFisher Scientific, Waltham, MA, USA), collected by centrifugation in the cold, and washed once with FACS buffer made by 10 mM 4-(2-hydroxyethyl)-1-piperazineethanesulfonic acid (HEPES) buffer at pH 7.4, 140 mM sodium chloride (NaCl) and 2.5 mM calcium chloride ($CaCl_2$). Cells were incubated with fluorochrome-conjugated antibodies (1:50 dilutions) in 50 μL of FACS buffer for 15 min in the dark. Cells were stained separately in each single screening tube with cluster of differentiation (CD)80-PE, CD163-PE and CD73-PE (all purchased by BD Biosciences, MA, USA) Then, the excess of antibodies was removed by adding fresh FACS buffer and centrifugation. After that, 20,000 events were run in a Beckman Coulter CytoFLEX flow cytometer (CA, USA). Relative fluorescence emissions of gated cells by forward and side scatter properties (FSC/SSC) were analyzed using the CytExpert Software (Beckman Coulter) and expressed as the mean fluorescence intensity (MFI) ratio on the isotype control. Individual values obtained from three independent experiments (n = 3) were summarized as means and standard deviations.

2.10. Catalase activity

To indirectly assess oxidative stress occurrence, the analysis of the antioxidant enzyme catalase activity was carried out. For this purpose, the Amplex® Red Catalase Assay Kit was used (Molecular Probes, Invitrogen Corporation, CA, USA) as reported previously (Sancilio et al., 2018). The absorbance was measured at 560 nm in a microplate reader (Multiskan GO, Thermo Scientific, MA, USA). The results are typically plotted by subtracting the observed fluorescence from that of a no-catalase control (complete RPMI). Assessment of the relative catalase activity (mU/mL) was calculated using a curve generated with specific standards provided by the manufacturers. Values obtained (n = 6) were normalized on MTT data.

2.11. Lactate dehydrogenase (LDH assay)

To quantify the release of the LDH enzyme and thus to indirectly assess intracellular lactate production, the CytoTox 96® Non-Radioactive Assay (Promega Corporation, Fitchburg, WI) was performed. The assay quantitatively measures LDH, a stable cytosolic enzyme that is released upon cell lysis. Supernatants obtained from lysed and homogenized cells after treatments (50 μL) were pipetted in a 96 well plate with a flat bottom (Falcon®, Corning Incorporated, New York, NY, USA) and the volume was doubled adding the LDH reaction mixture. After 30 min of incubation at room temperature in the dark, 50 μL of stop solution were added and the optical density (O.D.) was measured at 490 and 690 nm and the obtained O.D. were normalized with the one related to MTT. Next, the obtained O.D. from CTRL was set as 1 and data were shown as the fold increase on the CTRL. Individual values obtained from three independent experiments (n = 6) were summarized as means and standard deviations.

2.12. Statistics

Statistics were performed using the one-way analysis of variance (ANOVA) followed by the Tukey's multiple comparison test by means of the Prism 5.0 software (GraphPad, San Diego, CA, USA). Results are the mean values ± standard deviations. Values of $p \leq 0.05$ were considered statistically significant.

3. Results

3.1. Evaluation of cell metabolic activity (MTT test)

Differentiated macrophages were exposed to Meloxicam (M) and to newly synthesized compounds, namely **1**, **2**, **3**, **4**, **5**, **6**, **7**, **8** and **9**, (1 and 10 μM), in the absence (grey bars) or in the presence (red bars) of LPS for 24 h (Fig. 2A and Figure S1 of the Supplementary Materials). Compounds **5** and **8** have been selected based on previous data obtained from

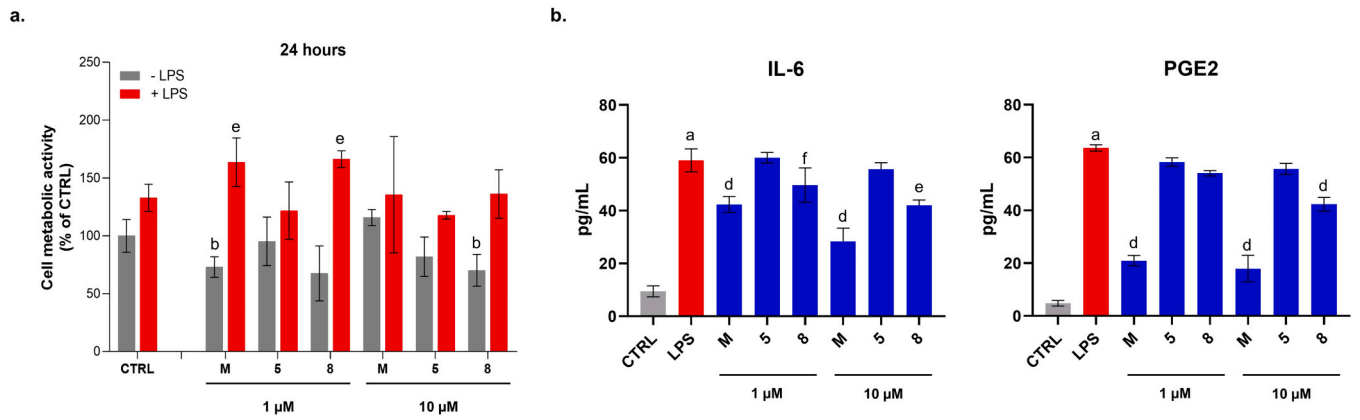

Fig. 2. (a) Cell metabolic activity of LPS-unstimulated (grey bars) and LPS-stimulated (red bars) human differentiated macrophages treated for 24 h with Meloxicam (M) and compounds **5 and 8** administered at 1 μM and 10 μM. Metabolic activity of untreated cells (CTRL without LPS, grey bar) was set as 100%. The red bar labelled as CTRL represents cells in the presence of LPS alone. (b) Interleukin (IL)-6 and prostaglandin E2 (PGE2) secretion from LPS-stimulated human macrophages in the presence of M, **5** and **8** at 1 and 10 μM after 24 h of exposure. Data are presented as the means ± standard deviations. a = $p<0.0001$ and b = $p<0.001$ between CTRL and compounds without LPS; d = $p<0.0001$, e = $p<0.001$ and f = $p<0.01$ between LPS and compounds with LPS.

in vitro experimentations on leukocyte functions (Bruni et al., 1993). Compound **8** was shown as a selective inhibitor of leukotrienes and/or prostaglandin biosynthesis in a dose-dependent manner in the range 1–100 μM, whereas **5** did not exhibit an anti-inflammatory activity in the same selection of concentrations. In this light, the authors chose to test a highly active compound compared to an ineffective one to further support the hypothesis that chemical moieties at position 2 are crucial to exert an anti-inflammatory activity.

Untreated cells were set as the control sample (CTRL, grey bar). Under non-inflammatory conditions, Meloxicam slightly but significantly decreases cell metabolic activity at 1 μM, while at 10 μM seems to be not effective. When **5** is added, a slight decrease of cell metabolic activity is registered at both concentrations. **8** significantly decreases cell metabolic activity at both concentrations. When cells are stimulated

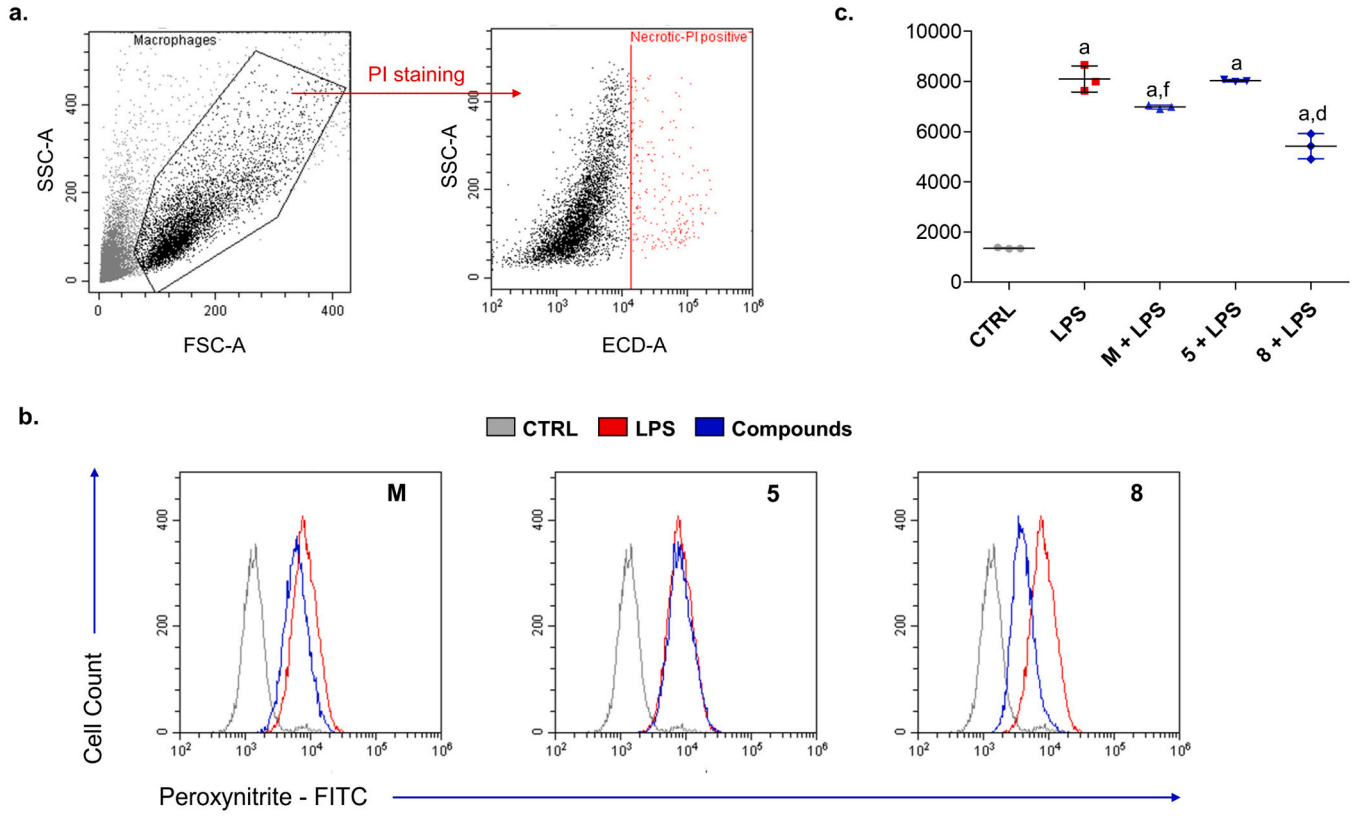

Fig. 3. Generation of peroxynitrite by LPS-stimulated human differentiated macrophages in the presence of Meloxicam (M) and compounds **5** and **8** at 10 μM after 24 h of exposure. (a) Gating strategy for the detection of peroxynitrite. Side scatter/Forward scatter (SSC/FSC) dot plots represent morphological parameters of unstained macrophages. Cells were incubated with Propidium iodide (PI) to assess the necrotic cell population. Cells PI-positive were gated and labelled ad necrotic. The cell population excluded from the logical gate "necrotic" represents viable macrophages and was used for further analyses. (b) Histograms were obtained by flow cytometry and are generated by plotting the cell count (y-axis) and the FITC fluorescence emission (x-axis). (c) The graph represents the fluorescence emission (MFI = Mean Fluorescence Factor) in the FITC channel which is proportional to the amount of peroxynitrite. Data are represented as means ± standard deviations. CTRL = untreated cells. LPS = 0.5 μg/mL LPS. a = $p<0.0001$ between CTRL and treated samples; d = $p<0.0001$ and f = $p<0.01$ between LPS alone and treated samples.

with LPS (pro-inflammatory conditions) and then exposed to **5** at 1 μM, a notable cell metabolic activity reduction is recorded compared to LPS-stimulated cells exposed to Meloxicam.

3.2. IL-6 and PGE2 secretion is reduced in the presence of 8

As expected, LPS-stimulated macrophages massively release IL-6 and PGE2 (59.01 pg/mL and 63.63 pg/mL, respectively) compared to cells under basal conditions (CTRL) (Fig. 2B). When Meloxicam is added, the IL-6 secretion and even more the PGE2 one are dramatically reduced compared to LPS alone, depending on the concentration. In parallel, **8** is significantly effective on both IL-6 and PGE2 production in a concentration-dependent manner, being amounts assessed at 42.56 pg/mL and 42.33 pg/mL, respectively, with 8 administered at 10 μM in LPS-stimulated macrophages. On the contrary, **5** is not effective.

3.3. Compound 8 decreases the amount of peroxynitrite in LPS-stimulated macrophages

The amount of intracellular peroxynitrite was measured to assess nitrosative stress occurrence under pro-inflammatory conditions and to evaluate its potential counteraction by compounds **5** and **8** in comparison with Meloxicam (Fig. 3). As expected, macrophages dramatically produce $ONOO^-$ in response to LPS (MFI = 8092) compared to basal conditions in untreated cells (MFI = 1348) (Fig. 3A). A notable right-shifted peak can be observed in the FITC channel (Fig. 3B). When Meloxicam is administered, the amount of $ONOO^-$ slightly but significantly decreases (MFI = 6978), whereas compound **5** seems not effective as regards peroxynitrite production. Notably, in the presence of **8** values of MFI registered are assessed to 5411 ($p<0.0001$), disclosing a significant reduction of generated $ONOO^-$.

3.4. Compounds 5 and 8 inhibit the exaggerated Nrf2 nuclear translocation in LPS-stimulated macrophages and positively modulate catalase activity

Then, considering that Nrf2 is a crucial transcription factor implicated in the recruitment of antioxidant pathways, its translocation in LPS-stimulated macrophages followed by treatment with Meloxicam, **5** and **8**, at 10 μM for 24 h, was evaluated by means of

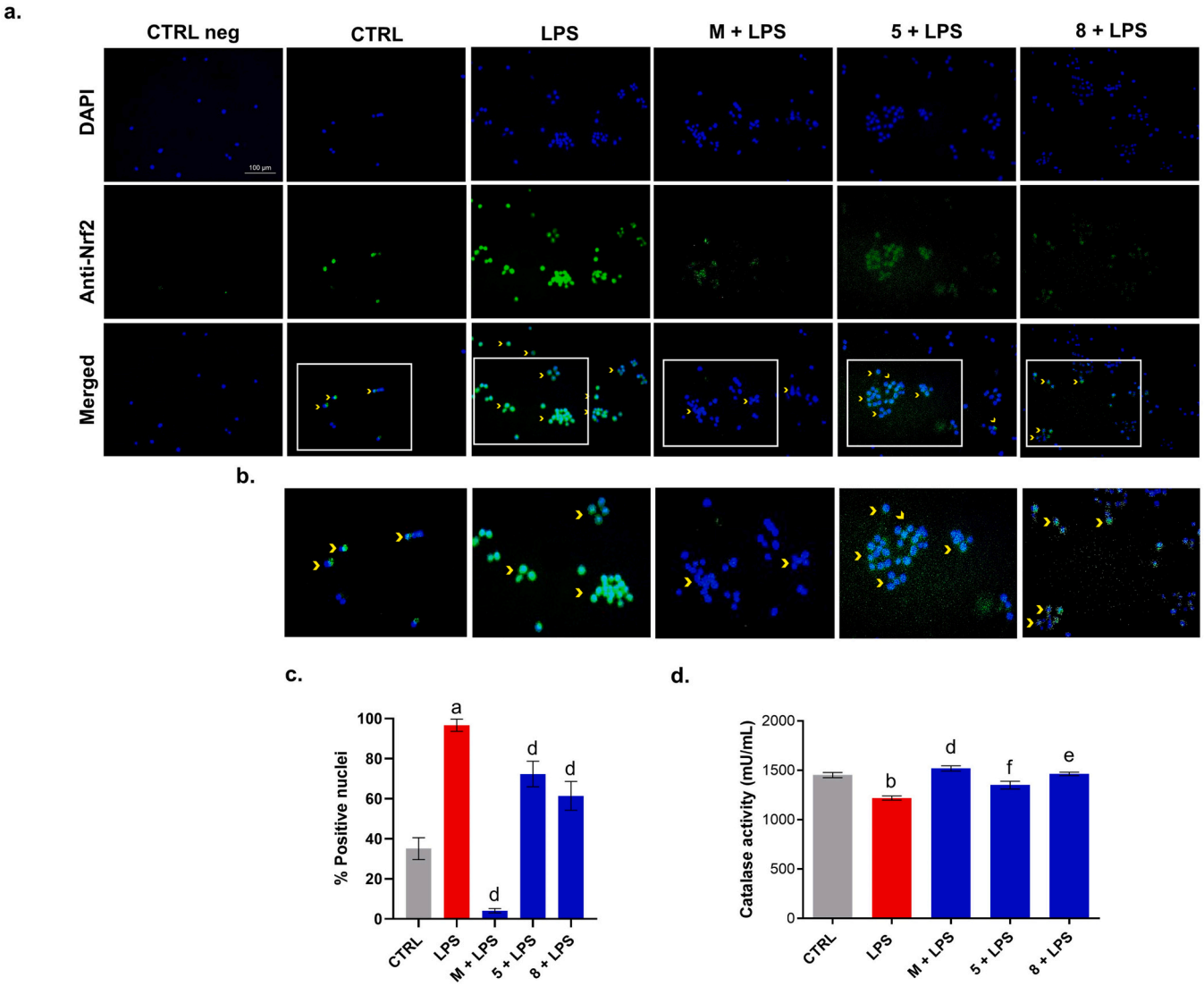

Fig. 4. Evaluation of the Nrf2 nuclear translocation and of catalase activity in LPS-stimulated human differentiated macrophages in the presence of Meloxicam (M) and compounds **5** and **8** at 10 μM after 24 h of exposure. (a) Representative images display cells stained positive for DAPI (nuclei), Nrf2 (green fluorescence) and the merge of the two fluorescence. Yellow arrows indicate cells stained positive for nuclear Nrf2. Magnification 10x. (b) Magnification of 10x images. (c) The bar graph shows the percentage of nuclei positive for Nrf2. (d) The bar graph shows the catalase activity rate expressed ad mU/mL normalized on MTT data. a = $p<0.0001$ and b = $p<0.001$ between CTRL and treated samples; d = $p<0.0001$, e = $p<0.001$ and f = $p<0.01$ between LPS alone and treated samples.

immunofluorescence and western blotting analyses (Fig. 4A-C). The analysis obtained with the Nrf2 immunofluorescence underlines that LPS-stimulated macrophages includes a higher number of Nrf2-positive cells compared to the other experimental conditions, and that the Nrf2 nuclear translocation rate is notably augmented in the same sample (Fig. 4A-B). When Meloxicam and **5** and **8** are administered in LPS-stimulated cells, the decrease of Nrf2 cell positivity is paralleled by a diminished nuclear translocation.

The activity of the antioxidant enzyme catalase was measured in the same experimental conditions (Fig. 4D). As expected, catalase activity slightly but significantly decreases in LPS-stimulated macrophages. On the contrary, Meloxicam, **5** and **8** restore the enzymatic activity in the presence of LPS. More in details, Meloxicam and **8** are more efficient of **5** in the counteraction of LPS-induced catalase decrease.

3.5. Modulation of the expression of surface markers associated to the polarization of macrophages

Expression levels of CD80 and CD163 were measured upon LPS-stimulation and in the presence of Meloxicam, **5**, and **8** by flow cytometry after 24 and 48 h (Fig. 5) to investigate the occurrence of polarization in macrophages. The immunophenotypic profile of undifferentiated monocytes was preliminary analysed to assess the occurrence of differentiation (see Figure S2 in the Supplementary). Monocytes from routine cultures are CD14 ^{pos} CD80 ^{neg} CD163 ^{neg} whereas differentiated macrophages *in vitro* by PMA are CD14 $^{high\ pos}$ CD80 $^{low\ pos}$ CD163 ^{neg}, in accordance with literature reporting an increase of CD14 upon PMA-differentiation (Jimenez-Duran et al., 2020).

After 24 h under basal conditions (CTRL), CD80 and CD163 expression levels are only hardly detectable (MFIs close to 1) (Fig. 5B). After the LPS stimulation, CD80 expression dramatically increases (MFI = 6.2), whereas the one related to CD163 is not affected. In the presence of Meloxicam, CD80 expression raises as well as CD163, although not in a significant manner. When **5** is administered, CD80 levels significantly decrease but not the ones of CD163. In parallel, in the presence of **8**, macrophages strongly express CD80 but not CD163.

After 48 h of exposure to treatments, levels of expression under basal conditions and in LPS-stimulated cells appears comparable to the ones registered at 24 h (Fig. 5C). Contrariwise, the presence of Meloxicam and even more of **8** significantly decreases CD80 expression levels with respect to LPS alone (MFI = 5.8 and 4.2, respectively). Compound **5** seems to be less effective than at 24 h, being the MFI related to CD80 augmented while the one related to CD163 is found decreased. Accordingly, percentages of positivity are reported in Table S1 of the Supplementary Materials.

3.6. Compound 8 decreases iNOS expression levels, increases TGFβ1 activation and modulates catalase activity in LPS-stimulated macrophages

Western blotting analysis was performed after LPS stimulation and

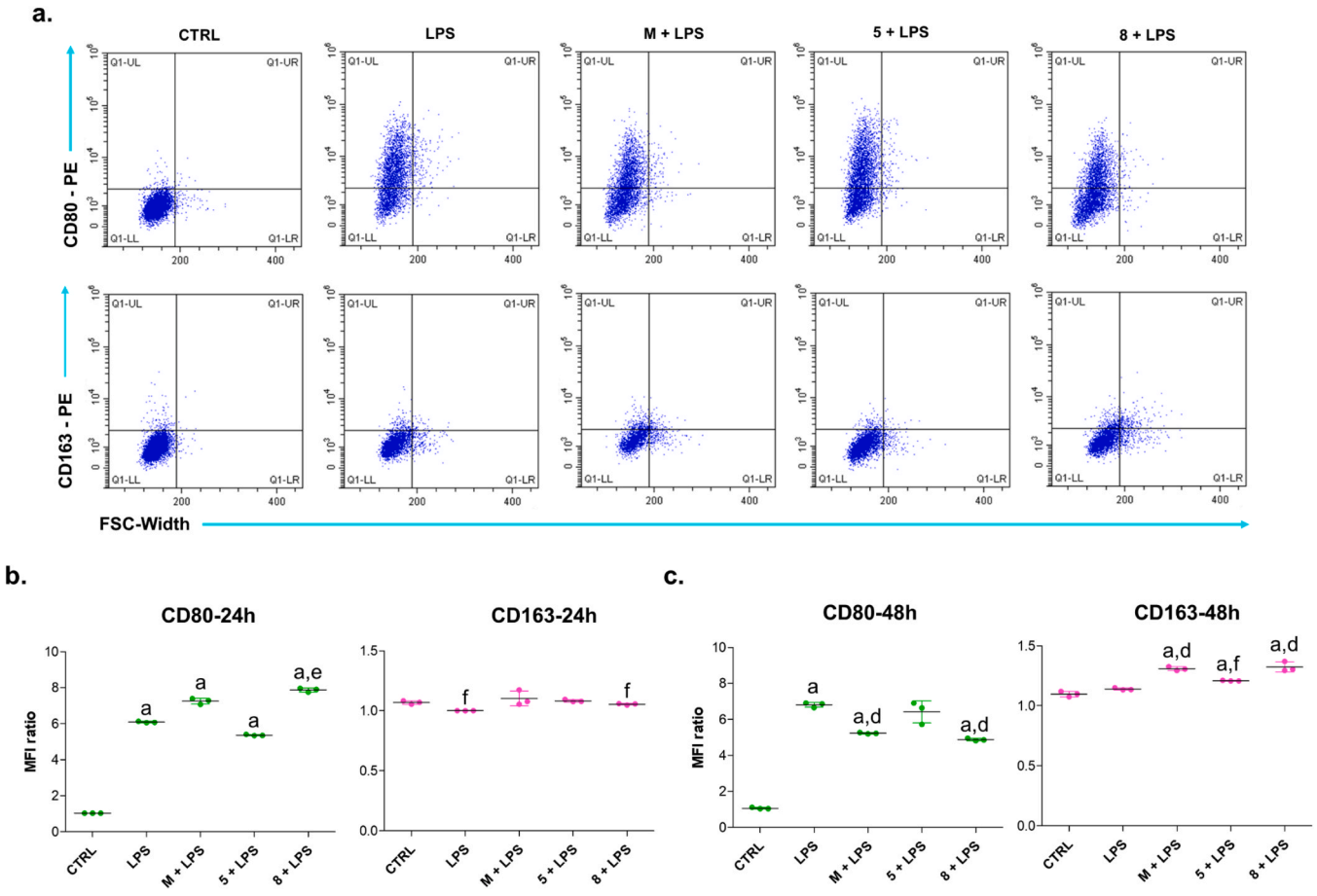

Fig. 5. Macrophage immunophenotype upon polarization of LPS-stimulated human differentiated macrophages in the presence of Meloxicam (M) and compounds **5** and **8** at 10 μM after 24 h of exposure. (a) Representative dot plots show the distribution of the cell population in response to treatments. Dot plots represent the population stained positive for CD80-PE or CD163-PE (y-axis) plotted towards the forward scatter (x-axis: FSC-Width). (b) Graphs show the mean fluorescence intensity (MFI) ratio obtained normalizing the fluorescence emission of the CD markers on the one obtained from the negative control (isotype control). CTRL = untreated cells. LPS = 0.5 μg/mL LPS. a = $p<0.0001$ between CTRL and treated samples; d = $p<0.0001$, e = $p<0.001$ and f = $p<0.01$ between LPS alone and treated samples.

exposure to Meloxicam and compounds to assess iNOS and TGFβ1 protein expression, a pro-inflammatory and an anti-inflammatory marker, respectively (Fig. 6A-B-C). The iNOS protein is well expressed in untreated human macrophages and in LPS-stimulated cells (Fig. 6A and B). When Meloxicam is added, the iNOS amount decreases. Notably, when LPS-stimulated macrophages are exposed to **5**, the iNOS is downregulated and this effect is even amplified in the presence of **8**. As for TGFβ1 expression (Fig. 6A and C), the amount of the full-length inactive protein (44 kDa) is found slightly increased only by the exposure to compound **8**. A 40 kDa band is detected only for LPS-stimulated macrophages, with or without Meloxicam and compounds. In the presence of LPS alone and when compound **8** is added, the protein detected slightly but significantly increased. In the low molecular weight range (25 kDa), another band can be detected for all the experimental conditions, as a sign of dimeric TGFβ1 presence. Again, the presence of LPS alone and when **8** is added to cultures, the dimeric TGFβ1 is upregulated in a major extent than in the presence of Meloxicam (M) and **5**.

Because Nrf2 transcripts for the antioxidant enzyme catalase which in turn neutralizes the intracellular hydrogen peroxide, its activity was quantified. As expected, the LPS decreases the activation of catalase (Fig. 6D). In the presence of Meloxicam, the highest increase in the catalse activity was registered, followed by exposures to **8** and **5**.

3.7. Compounds 5 and 8 upregulate CD73 expression levels and increase the amount of lactate released from LPS-stimulated macrophages

Membrane surface expression of CD73 on LPS-stimulated macrophages was measured after 24 h of treatments by flow cytometry (Fig. 7). Under basal conditions (CTRL), cells weakly express CD73 (Fig. 7B) as shown also by the distribution of cell population, which is grouped in the negative-stained cell quadrant (Fig. 7A). When macrophages are stimulated by LPS alone, CD73 levels increase (MFI = 1118). Cell exposure to M + LPS, **5** + LPS and **8** + LPS significantly increases CD73 expression compared to LPS alone (MFIs = 1442; 1450; 1614). A change is registered in the distribution of the cell population in these experimental conditions, being right-shifted in the positive-stained cell quadrant.

The amount of intracellular lactate produced was indirectly measured as the released of the LDH enzyme endogenously produced by macrophages exposed to treatments (Fig. 7C). The amount of LDH released upon total cell lysis is comparable to the one in the control sample for all the experimental conditions, except for a dramatic increase as regards LPS-stimulated macrophages in the presence of **8** both at 24 and 48 h.

4. Discussion

Macrophages are specialized cells involved in detection, phagocytosis and destruction of bacteria and other harmful organisms. They undergo activation by pathophysiological stimuli to undergo towards a pro-inflammatory and bactericidal (M1) phenotype or a wound healing and anti-inflammatory (M2) one. Dysregulation of the M1/M2 balance is often associated with inflammatory diseases and pre-cancerous lesions. To establish optimized and reliable macrophage-based cell models for the screening of new compounds and to analyze mechanisms of macrophage polarization and related signaling pathways may reveal new drug targets (Shiratori et al., 2018). In this light, differentiated human macrophages from blood monocytes were used here as the experimental model. Differentiation was carried out following a well-established procedure which employs the administration of sub-toxic concentrations of PMA, which, in turn, triggers the NF-κB translocation and activate monocytes (Daigneault et al., 2010; Lasalvia et al., 2022). The LPS was then used as the inflammatory stimulus, being able to amplify the NF-κB signal, which transcripts for the iNOS and triggers the release of pro-inflammatory cytokines such as TNFα (Schweikl et al., 2021). Since they were found able to inhibit leukotrienes and/or prostaglandin biosynthesis by modulating the superoxide production and the myeloperoxidase release, compounds **1**-**9** were afterwards administered at 1 and 10 μM in the established inflamed environment *in vitro*.

Reprogramming of intracellular metabolism is required for the proper polarization and function of activated macrophages. LPS-stimulated M1 macrophages increase glucose consumption and lactate release to meet their augmented energy requirement (Alghamdi et al., 2022), thus resulting in an augmented colorimetric signal measured by the MTT assay. In this light, cell metabolic activity, IL-6 and PGE2 secretion of LPS-unstimulated or stimulated macrophages in the presence of **5** and **8** and Meloxicam was firstly measured (Fig. 2A-B). Our data reveal that almost all the compounds are biocompatible and do not activate macrophages at the tested concentrations. Under pro-inflammatory conditions, **5** succeeds at counteracting LPS-induced increased cell metabolic activity. In parallel, compound **8** seems not effective in the presence of LPS but discloses a low activity level under basal conditions. As for IL-6 and PGE2 secretion, **8** is the best compound in decreasing amounts, therefore disclosing the best anti-inflammatory activity. **5** and **8** contain an aromatic ring aryl and its bioisosteric thiophene respectively, thus corroborating the importance of this kind of substitution at C2 position as previously demonstrated (Bruni et al., 1993). In the same work, it has been reported that **8** was capable of inhibiting leukotrienes and/or prostaglandin biosynthesis in a dose-dependent manner in the concentration range 1–100 μM, whereas **5** did not exhibit an anti-inflammatory activity in the same selection of

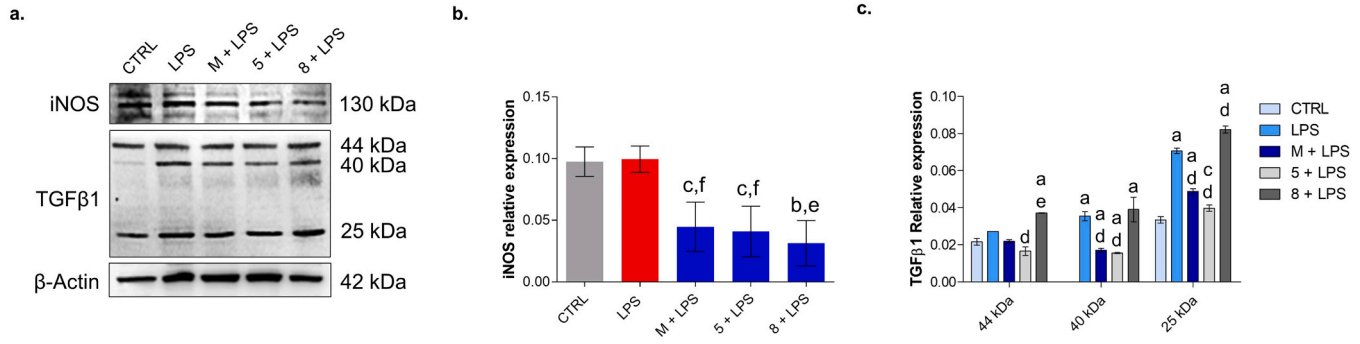

Fig. 6. iNOS and TGFβ1 levels of protein expression and catalase activity in LPS-stimulated human differentiated macrophages in the presence of Meloxicam (M) and compounds **5** and **8** at 10 μM after 24 h of exposure. (a) Western blot analysis of iNOS (130 kDa) and TGFβ1 (44–25 kDa). β-Actin (42 kDa) was used as loading control. (b-c) Bar graphs display densitometric values related to protein levels expressed as mean densitometric measurements ± standard deviations (n = 3) normalized on the ones of the loading control. a = $p<0.0001$, b = $p<0.001$ and c = 0.01 between CTRL and treated samples; d = $p<0.0001$, e = $p<0.001$ and f = $p<0.01$ between LPS alone and treated samples.

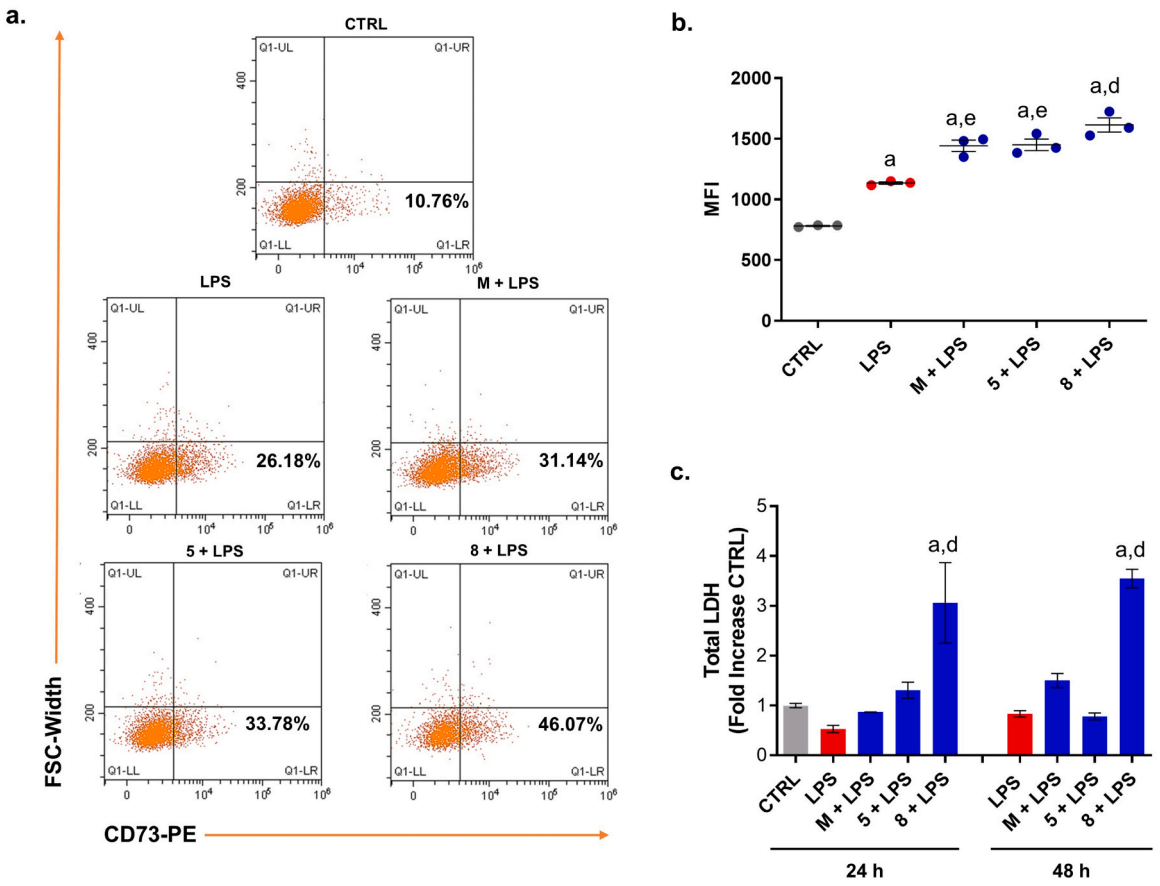

Fig. 7. CD73 expression in LPS-stimulated human differentiated macrophages in the presence of Meloxicam (M) and compounds **5** and **8** at 10 μM after 24 h of exposure. (a) Representative dot plots show the distribution of the cell population in response to treatments. Dot plots represent the population stained positive for CD73-PE (x-axis) plotted towards the forward scatter (y-axis: FSC-Width). Representative percentages of CD73 positive cells are shown in the lower-right quadrant. (b) The graph represents the mean fluorescence emission (MFI = mean fluorescence intensity) in the PE channel which is proportional to the amount of CD73 on cell surfaces. (c) The bar graph shows the release of total LDH from each sample. Values are the fold increases of untreated cells (CTRL). Data are represented as means ± standard deviations. a = $p<0.0001$ between CTRL and treated samples; d = $p<0.0001$ and e = $p<0.001$ between LPS alone and treated samples.

concentrations. In this light, the authors chose to test a highly active compound (**8**) compared to an ineffective one (**5**) to further support the hypothesis that substituents at position 2 are crucial to exert the anti-inflammatory activity. For these reasons, **5** and **8** were used for further analyses which were run out only under pro-inflammatory conditions (LPS stimulation).

The formation of RNS in inflamed macrophages is mostly the result of the enhanced NFκB-regulated expression of NADPH oxidase 2 (Nox2) and iNOS enzymes triggered by pro-inflammatory stimuli such as LPS. Activation of Nox2 and iNOS enhances the formation of superoxide anions and nitric oxide ($NO^{\bullet}$), which combine to $ONOO^-$ to finally build an overabundance of ROS and RNS (Singel and Segal, 2016). In our experimental model, the amount of intracellular $ONOO^-$ is considerably increased in LPS-stimulated cells, whereas Meloxicam and compounds are effective in decreasing RNS, mainly **8** (Fig. 3). It has been demonstrated that the downregulation of LPS-stimulated inflammation occurs under the NFκB-induced expression of the antioxidant protein HO-1 (heme oxygenase 1), which protects cells both from oxidative and nitrosative stress (Vijayan et al., 2018 Jul). HO-1 synthesis and activation is Nrf2-dependent (Loboda et al., 2016) and thus the modulation of LPS-induced $ONOO^-$ production in macrophages is controlled through the activation of the Nrf2 system and its crosstalk with the NFκB signaling (Sancilio et al., 2018). Therefore, the analysis of the Nrf2 translocation was carried out in our experimental model (Fig. 4). Immunofluorescence data reveal that Nrf2 is strongly translocated by the LPS-stimulation. As already reported, Nrf2 levels were drastically boosted in cell nuclei as a result of RNS production (Schweikl et al., 2021). The reduction of nitrosative stress in LPS-stimulated cells induced by Meloxicam, **5** and mainly **8** might justify the nuclear reduced expression of Nrf2 in the same experimental conditions, although Nrf2 expression levels are maintained high and comparable to the ones registered in the presence of LPS alone. Moreover, a more detailed observation of the immunofluorescence staining reveals that, in the presence of LPS alone, the Nrf2-FITC fluorescence is homogenous and predominant in the nucleus while in the presence of Meloxicam, **5** and **8** Nrf2 positive cells are still present, but the staining seems more punctuate and perinuclear. Test compounds are also able to increase the activity rate of the antioxidant enzyme catalase, which is directly transcript by Nrf2 under pro-oxidant conditions (Gallorini et al., 2015). LPS-induced macrophage polarization leads to a considerable decline in the catalase level, which may help to maintain increased H_2O_2 concentration inside cells. In macrophages, elevated levels of H_2O_2 act as a pathogen-killing agent when converted to hypochlorous acid. The excessive production of H_2O_2 in M1 macrophages is mainly assigned to NADPH oxidase(s), which become active in response to stimulation of TLRs by LPS. The hyperreactive superoxide anion released by NADPH oxidese(s) is immediately converted to a more stable and membrane permeable molecule (H_2O_2) (Sobczak et al., 2021). In parallel, the accumulation of H_2O_2 and the LPS-induced nitrosative stress stimulates Nrf2 activation as widely reported (Gallorini et al., 2023).

In this scenario it is plausible to assume that Nrf2 is activated and translocated by LPS in macrophages but this activation it is not translated into an oxidative stress counteraction. On the contrary, a down-regulation of Nrf2 in LPS-stimulated cells by Meloxicam and compounds

is effective, because Nrf2 is still efficiently maintained expressed to levels capable of activating the antioxidant machinery and thus to protect cells from the nitrosative/oxidative stress.

In the same experimental conditions, an increase in the $CD163^+$ cell population and a decrease in the $CD80^-$ one is registered after 48 h of exposures (Fig. 5). CD163 is a macrophage specific scavenger receptor for haptoglobin-hemoglobin complexes found on the cell membranes of M2 macrophages. Its expression is strongly induced by the anti-inflammatory cytokine IL-10, making CD163 a marker of the anti-inflammatory process occurrence (Rasmussen and Etzerodt, 2021). On the contrary, $CD80^+$ cells are classically M1 macrophages (Yilmaz et al., 2022). Our data therefore demonstrate that CD163 increased expression triggered by **8** is comparable with the one induced by the reference compound Meloxicam. Additionally, in the same experimental conditions, **8** is capable of downregulating the iNOS (Fig. 6A), thus corroborating our data on *in silico* prediction analyses, peroxynitrite generation and immunophenotyping results regarding the M1 marker CD80, being the iNOS a pro-inflammatory marker itself (Jiménez-Uribe et al., 2019). In parallel, the anti-inflammatory protein TGFβ1 is activated by test compounds and Meloxicam, mainly in the presence of **8**, as a sign of an anti-inflammatory cell response occurrence (Kao et al., 2020). It has been already reported a mutual inter-regulation between iNOS and TGFβ1 which is one of the most potent cytokine regulating iNOS under physiological and pathological conditions (Abd El-Aleem et al., 2020). It has been therefore reported that TGFβ1 suppresses IFN-gamma-induced NO production in macrophages by suppressing STAT1 activation and accelerating iNOS protein degradation (Takaki et al., 2006).

Regulation of redox equilibrium and metabolic pathways are tightly connected functions within the human body. During the past decade, numerous studies have highlighted that metabolic pathways determine cell fate and function of immunocompetent cells, giving rise to an area of research referred to as immunometabolism (Muri and Kopf, 2021). In this scenario, the role of Nrf2 is likely context dependent. It has been reported that *Nrf2* deficiency increases type 2 cytokine responses and airway inflammation in an asthma model (Rangasamy et al., 2005 Jul 4). In another work, Nrf2 translocation was found responsible for the increasing of TH2 cytokine secretion by inducing interferon-γ (IFNγ)-mediated responses (Rockwell et al., 2012 Feb 15). Recently, it has been demonstrated a role for the Nrf2 molecular axis in the regulation of metabolism and inflammatory properties of T cells in children with rheumatism (Rajendiran et al., 2022). In our model, the experimental condition showing the best Nrf2 modulation and the best increase in anti-inflammatory parameters (i.e. nuclear translocation, increased Nrf2 expression levels in cytosol, high number of positive cells revealed by immunofluorescence, increase in the $CD163^+$ population, catalase activity rate increased, iNOS downregulation and TGFβ1 upregulation) is the exposure to compound **8**, followed by exposure to Meloxicam and **5**. Upon these treatments, CD73 expression is reported considerably high (Fig. 7A). Moreover, the content of lactate dehydrogenase (LDH) after total cell lysis upon exposure to **8** is considerably high. Although aware of the limitation of the technique, the amount of LDH from lysed cells after treatments can indirectly measure intracellular lactate, being lactate produced from the reaction between pyruvate and lactate dehydrogenase.

Recently we have demonstrated that the expression of the 5'-ectonucleotidase CD73 was increased in a previously established cell model of inflammation, where pulp cells were LPS-stimulated to induce iNOS expression (Cataldi et al., 2022). It is reported that CD73-triggered signal stimulates a shift from an ATP-driven pro-inflammatory environment to an anti-inflammatory niche induced by adenosine in macrophages, making this protein an interesting target for the immunotherapy of inflammatory diseases (Murphy et al., 2017). Recent studies from cancer research highlighted that tumor-derived lactate, known as Warburg effect, has immunosuppressive effects on immune cells (Colegio et al., 2014). Additional studies have revealed that lactate suppresses macrophage pro-inflammatory response to LPS-stimulation by inhibiting NFκB (Manoharan et al., 2021). Upon the Warburg effect, CD73 has been found to be a crucial player (Cao et al., 2021). Additionally, the implication in the anti-inflammatory signaling of a CD73-triggered molecular axis (Xu et al., 2021; Gao et al., 2022).

5. Conclusions

A series of 9 4,7-dihydro-4-ethylpyrazolo[*l*,5-*a*]pyrimidin-7-ones was here tested in comparison to Meloxicam in a cell model of inflammation, where macrophages were stimulated with LPS. Two selected compounds (**5** and **8**) from the cell metabolic activity assay were furthermore tested to demonstrate their potential as anti-inflammatory compounds. Our data reveal that, differently from compound **5**, the most effective compound is **8**, owning an anti-inflammatory profile comparable to the one of Meloxicam in terms of counteraction of nitrosative stress, Nrf2 nuclear translocation modulation, activation and expression of the CD163 marker, iNOS inhibition, TGFβ1 upregulation and catalase activity increase. Our work furthermore highlights that the counteraction of the LPS-induced inflammation by **8** is related to the triggering of CD73, which could regulate a crucial signaling in the anti-inflammatory cascade in macrophages acting also on their metabolic machinery. These intriguing results highlight a potential innovative target for compound **8** and lay the ground for further investigations for this compound as an immunomodulator. Additionally, the clinical management of inflammatory-related diseases is still a challenge. There is always need for an alternative to NSAIDs, known to be characterized by a high potency but long-term side effects. In this light, compounds active on immunomodulatory targets might be an alternative to canonical anti-inflammatory drugs.

Funding

This work was supported by local grants from the Italian Ministry of University and Research held by M.G. and S.C (FAR2021).

Author statement

The authors declare non competing interests. All the authors have read and approved the final version of the manuscript.

CRediT authorship contribution statement

Susi Zara: Formal analysis, Methodology. **Alessia Ricci:** Methodology, Formal analysis, Writing – original draft. **Valentina Di Valerio:** Methodology, Formal analysis. **Fabrizio Carta:** Data curation, Investigation, Writing – original draft. **Silvia Sancilio:** Writing – original draft, Methodology, Data curation. **Silvia Selleri:** Writing – original draft, Methodology, Investigation, Writing – review & editing. **Amelia Cataldi:** Writing – review & editing, Resources, Funding acquisition. **Simone Carradori:** Writing – review & editing, Writing – original draft, Resources, Project administration, Investigation, Funding acquisition. **Claudiu T. Supuran:** Writing – review & editing, Validation, Resources, Funding acquisition. **Marialucia Gallorini:** Writing – review & editing, Resources, Project administration, Investigation, Conceptualization, Supervision, Validation, Writing – original draft.

Data Availability

Data are available within the manuscript.

Appendix A. Supporting information

Supplementary data associated with this article can be found in the online version at doi:10.1016/j.molimm.2024.04.004.

References

Abd El-Aleem, S.A., Mohammed, H.H., Saber, E.A., Embaby, A.S., Djouhri, L., 2020. Mutual inter-regulation between iNOS and TGF-β1: Possible molecular and cellular mechanisms of iNOS in wound healing. Biochim Biophys. Acta Mol. Basis Dis. 1866 (10), 165850.

Alghamdi, M., Gutierrez, J., Komarnytsky, S., 2022. Essential minerals and metabolic adaptation of immune cells. Nutrients 15 (1), 123.

Bruni, F., Costanzo, A., Selleri, S., Guerrini, G., Fantozzi, R., Pirisino, R., Brunelleschi, S., 1993. Synthesis and study of the anti-inflammatory properties of some pyrazolo[1,5-a]pyrimidine derivatives. J. Pharm. Sci. 82 (5), 480–486.

Cao, X., Zhu, Z., Cao, Y., Hu, J., Min, M., 2021. CD73 is a hypoxia-responsive gene and promotes the Warburg effect of human gastric cancer cells dependent on its enzyme activity. J. Cancer 12 (21), 6372–6382.

Cataldi, A., Amoroso, R., di Giacomo, V., Zara, S., Maccallini, C., Gallorini, M., 2022. The inhibition of the inducible nitric oxide synthase enhances the DPSC mineralization under LPS-induced inflammation. Int J. Mol. Sci. 23 (23), 14560.

Chiu, S., Bharat, A., 2016. Role of monocytes and macrophages in regulating immune response following lung transplantation. Curr. Opin. Organ Transpl. 21 (3), 239–245.

Colegio, O.R., Chu, N.Q., Szabo, A.L., Chu, T., Rhebergen, A.M., Jairam, V., et al., 2014. Functional polarization of tumour-associated macrophages by tumourderived lactic acid. Nature 513 (7519), 559–563.

Daigneault, M., Preston, J.A., Marriott, H.M., Whyte, M.K., Dockrell, D.H., 2010. The identification of markers of macrophage differentiation in PMA-stimulated THP-1 cells and monocyte-derived macrophages. PLoS One 5 (1), e8668.

Daina, A., Michielin, O., Zoete, V., 2019. SwissTargetPrediction: updated data and new features for efficient prediction of protein targets of small molecules. Nucleic Acids Res 47 (W1), W357–W364.

Gallorini, M., Carradori, S., Panieri, E., Sova, M., Saso, L., 2023. Modulation of NRF2: biological dualism in cancer, targets and possible therapeutic applications. Sep 6 Antioxid. Redox Signal. https://doi.org/10.1089/ars.2022.0213.

Gallorini, M., Carradori, S., Resende, D.I.S.P., Saso, L., Ricci, A., Palmeira, A., Cataldi, A., Pinto, M., Sousa, E., 2022. Natural and synthetic xanthone derivatives counteract oxidative stress via Nrf2 modulation in inflamed human macrophages. Int J. Mol. Sci. 23 (21), 13319.

Gallorini, M., Petzel, C., Bolay, C., Hiller, K.A., Cataldi, A., Buchalla, W., Krifka, S., Schweikl, H., 2015. Activation of the Nrf2-regulated antioxidant cell response inhibits HEMA-induced oxidative stress and supports cell viability. Biomaterials 56, 114–128.

Gao J., Chen S., Kong T., Wen D., Yang Q. The relationship between soluble CD73 and the incidence of septic shock in severe sepsis patients: a cross-sectional analysis of data from a prospective FINNAKI study. Ann Transl Med. 2022;10(6):302.koll.

Hassanshahi, A., Moradzad, M., Ghalamkari, S., Fadaei, M., Cowin, A.J., Hassanshahi, M., 2022. Macrophage-mediated inflammation in skin wound healing. Cells 11 (19), 2953. https://doi.org/10.3390/cells11192953.

Jimenez-Duran, G., Luque-Martin, R., Patel, M., Koppe, E., Bernard, S., Sharp, C., Buchan, N., Rea, C., de Winther, M.P.J., Turan, N., Angell, D., Wells, C.A., Cousins, R., Mander, P.K., Masters, S.L., 2020. Pharmacological validation of targets regulating CD14 during macrophage differentiation. EBioMedicine 61, 103039.

Jiménez-Uribe, A.P., Valencia-Martínez, H., Carballo-Uicab, G., Vallejo-Castillo, L., Medina-Rivero, E., Chacón-Salinas, R., Pavón, L., Velasco-Velázquez, M.A., Mellado-Sánchez, G., Estrada-Parra, S., Pérez-Tapia, S.M., 2019. CD80 expression correlates with IL-6 production in THP-1-like macrophages costimulated with LPS and dialyzable leukocyte extract (Transferon®). J. Immunol. Res 2019, 2198508.

Kao, J.K., Wang, S.C., Ho, L.W., Huang, S.W., Lee, C.H., Lee, M.S., Yang, R.C., Shieh, J.J., 2020. M2-like polarization of THP-1 monocyte-derived macrophages under chronic iron overload. Ann. Hematol. 99 (3), 431–441. https://doi.org/10.1007/s00277-020-03916-8.

Khalil, N.Y., Aldosari, K.F., 2020. Meloxicam. Profiles Drug Subst. Excip. Relat. Method. 45, 159–197.

Kobayashi, E.H., Suzuki, T., Funayama, R., Nagashima, T., Hayashi, M., Sekine, H., Tanaka, N., Moriguchi, T., Motohashi, H., Nakayama, K., Yamamoto, M., 2016. Nrf2 suppresses macrophage inflammatory response by blocking proinflammatory cytokine transcription. Nat. Commun. 7, 11624.

Kolliniati, O., Ieronymaki, E., Vergadi, E., Tsatsanis, C., 2022. Metabolic regulation of macrophage activation. J. Innate Immun. 14 (1), 51–68. https://doi.org/10.1159/000516780.

Lasalvia, A., Cairone, F., Cesa, S., Maccelli, A., Crestoni, M.E., Menghini, L., Carradori, S., Marinacci, B., Gallorini, M., Elsallabi, O., Pesce, M., Patruno, A., 2022. Characterization and valorization of 'sulmona red garlic' peels and small bulbs. Antioxidants 11 (11), 2088.

Li, X., Teng, L., Yang, Z., 2022. Editorial: from chronic inflammation to cancer: how far can immunotherapy go? Front Pharm. 12, 838917.

Loboda, A., Damulewicz, M., Pyza, E., Jozkowicz, A., Dulak, J., 2016. Role of Nrf2/HO-1 system in development, oxidative stress response and diseases: an evolutionarily conserved mechanism. Cell Mol. Life Sci. 73 (17), 3221–3247.

Manoharan, I., Prasad, P.D., Thangaraju, M., Manicassamy, S., 2021. Lactate-dependent regulation of immune responses by dendritic cells and macrophages. Front Immunol. 12, 691134.

Muri, J., Kopf, M., 2021. Redox regulation of immunometabolism. Nat. Rev. Immunol. 21 (6), 363–381.

Murphy, P.S., Wang, J., Bhagwat, S.P., Munger, J.C., Janssen, W.J., Wright, T.W., Elliott, M.R., 2017. CD73 regulates anti-inflammatory signaling between apoptotic cells and endotoxin-conditioned tissue macrophages. Cell Death Differ. 24 (3), 559–570.

Naito, Y., Takagi, T., Higashimura, Y., 2014. Heme oxygenase-1 and anti-inflammatory M2 macrophages. Arch. Biochem Biophys. 564, 83–88.

Nguyen, T., Nioi, P., Pickett, C.B., 2009. The Nrf2-antioxidant response element signaling pathway and its activation by oxidative stress. J. Biol. Chem. 284 (20), 13291–13295.

Papalexi, E., Satija, R., 2018. Single-cell RNA sequencing to explore immune cell heterogeneity. Nat. Rev. Immunol. 18 (1), 35–45.

Rajendiran, A., Subramanyam, S.H., Klemm, P., Jankowski, V., van Loosdregt, J., Vastert, B., Vollbach, K., Wagner, N., Tenbrock, K., Ohl, K., 2022. NRF2/Itaconate axis regulates metabolism and inflammatory properties of T cells in children with JIA. Antioxidants 11 (12), 2426.

Rangasamy, T., Guo, J., Mitzner, W.A., Roman, J., Singh, A., Fryer, A.D., Yamamoto, M., Kensler, T.W., Tuder, R.M., Georas, S.N., Biswal, S., 2005 Jul 4. Disruption of Nrf2 enhances susceptibility to severe airway inflammation and asthma in mice. J. Exp. Med 202 (1), 47–59.

Rasmussen, R.K., Etzerodt, A., 2021. Therapeutic targeting of tumor-associated macrophages. Adv. Pharm. 91, 185–211.

Rockwell, C.E., Zhang, M., Fields, P.E., Klaassen, C.D., 2012 Feb 15. Th2 skewing by activation of Nrf2 in CD4(+) T cells. J. Immunol. 188 (4), 1630–1637.

Rodríguez-Prados, J.C., Través, P.G., Cuenca, J., Rico, D., Aragonés, J., Martín-Sanz, P., Cascante, M., Boscá, L., 2010. Substrate fate in activated macrophages: a comparison between innate, classic, and alternative activation. J. Immunol. 185 (1), 605–614.

Sancilio, S., Gallorini, M., Di Nisio, C., Marsich, E., Di Pietro, R., Schweikl, H., Cataldi, A., 2018. Alginate/hydroxyapatite-based nanocomposite scaffolds for bone tissue engineering improve dental pulp biomineralization and differentiation. Stem Cells Int 2018, 9643721.

Sancilio, S., Marsich, E., Schweikl, H., Cataldi, A., Gallorini, M., 2019. Redox control of IL-6-mediated dental pulp stem-cell differentiation on alginate/hydroxyapatite biocomposites for bone ingrowth. Nanomaterials 9 (12), 1656.

Schweikl, H., Birke, M., Gallorini, M., Petzel, C., Bolay, C., Waha, C., Hiller, K.A., Buchalla, W., 2021. HEMA-induced oxidative stress inhibits NF-κB nuclear translocation and TNF release from LTA- and LPS-stimulated immunocompetent cells. Dent. Mater. 37 (1), 175–190.

Shapouri-Moghaddam, A., Mohammadian, S., Vazini, H., Taghadosi, M., Esmaeili, S.A., Mardani, F., Seifi, B., Mohammadi, A., Afshari, J.T., Sahebkar, A., 2018. Macrophage plasticity, polarization, and function in health and disease. J. Cell Physiol. 233 (9), 6425–6440.

Shiratori, H., Feinweber, C., Luckhardt, S., Wallner, N., Geisslinger, G., Weigert, A., Parnham, M.J., 2018. An in vitro test system for compounds that modulate human inflammatory macrophage polarization. Eur. J. Pharm. 833, 328–338.

Singel, K.L., Segal, B.H., 2016. NOX2-dependent regulation of inflammation. Clin. Sci. (Lond.) 130 (7), 479–490.

Sobczak, M., Strachowska, M., Gronkowska, K., Karwaciak, I., 2021. LSD1 facilitates pro-inflammatory polarization of macrophages by repressing catalase. Cells 10 (9), 2465.

Takaki, H., Minoda, Y., Koga, K., Takaesu, G., Yoshimura, A., Kobayashi, T., 2006. TGF-beta1 suppresses IFN-gamma-induced NO production in macrophages by suppressing STAT1 activation and accelerating iNOS protein degradation. Genes Cells 11 (8), 871–882.

Tang, K., Zhang, J., Cao, H., Xiao, G., Wang, Z., Zhang, X., Zhang, N., Wu, W., Zhang, H., Wang, Q., Xu, H., Cheng, Q., 2022. Identification of CD73 as a novel biomarker encompassing the tumor microenvironment, prognosis, and therapeutic responses in various cancers. Cancers 14 (22), 5663.

Vijayan, V., Wagener, F.A.D.T.G., Immenschuh, S., 2018 Jul. The macrophage heme-heme oxygenase-1 system and its role in inflammation. Biochem Pharm. 153, 159–167.

Wang, L., He, C., 2022. Nrf2-mediated anti-inflammatory polarization of macrophages as therapeutic targets for osteoarthritis. Front. Immunol. 13, 967193.

Xu, S., Wang, J., Zhong, J., Shao, M., Jiang, J., Song, J., Zhu, W., Zhang, F., Xu, H., Xu, G., Zhang, Y., Ma, X., Lyu, F., 2021. CD73 alleviates GSDMD-mediated microglia pyroptosis in spinal cord injury through PI3K/AKT/Foxo1 signaling. Clin. Transl. Med 11 (1), e269.

Yilmaz, M., Demir, E., Firatli, Y., Firatli, E., Gürsoy, U.K., 2022. Tissue levels of CD80, CD163 and CD206 and their ratios in periodontal and peri-implant health and disease. Curr. Issues Mol. Biol. 44 (10), 4704–4713.

Yu, Q., Wang, Y., Dong, L., He, Y., Liu, R., Yang, Q., Cao, Y., Wang, Y., Jia, A., Bi, Y., Liu, G., 2020. Regulations of glycolytic activities on macrophages functions in tumor and infectious inflammation. Front. Cell Infect. Microbiol 10, 287.

Yunna, C., Mengru, H., Lei, W., Weidong, C., 2020. Macrophage M1/M2 polarization. Eur. J. Pharm. 877, 173090.